Microwave Dielectric Properties of Flexible Butyl Rubber–Strontium Cerium Titanate Composites

Chameswary Janardhanan,[1] Dhanesh Thomas,[1] Ganesanpotti Subodh,[1] Soumya Harshan,[2] Jacob Philip,[2] Mailadil T. Sebastian[1]

[1]*Materials Division, National Institute for Interdisciplinary Science and Technology, CSIR, Trivandrum, India 695019*
[2]*Department of Instrumentation and STIC, Cochin University of Science and Technology, Cochin 682022, India*

Received 1 February 2011; accepted 27 July 2011
DOI 10.1002/app.35364
Published online 21 November 2011 in Wiley Online Library (wileyonlinelibrary.com).

ABSTRACT: Butyl rubber–strontium cerium titanate (BS) composites have been prepared by hot pressing. The tensile tests show that the BS composites are flexible. The dielectric properties of the composites have been investigated at 1 MHz and 5 GHz as a function of ceramic contents. The composite with volume fraction 0.43 of ceramic filler has a dielectric constant (ε_r) of 11.9 and dielectric loss (tan δ) 1.8×10^{-3} at 5 GHz. The measured values of ε_r are compared with the effective values calculated using different theoretical models. The thermal conductivity of the composites is found to increase with ceramic contents and reaches a value of 4.5 Wm^{-1} K^{-1} for maximum filler loading 0.43 volume fraction. The coefficient of thermal expansion of the composites decreases gradually with filler loading and reaches a minimum value of 30.2 ppm $°C^{-1}$ at a volume fraction 0.43. © 2011 Wiley Periodicals, Inc. J Appl Polym Sci 124: 3426–3433, 2012

Key words: composites; microstructure; mechanical properties; matrix; thermal properties

INTRODUCTION

Flexible dielectric substrates play an important role in the electronic industry. Compared to flexible electronics built on nonstretchable materials, stretchable materials offer a wide range of advantages such as ability to reduce package size and weight, cost effective installation, and dissipation of heat at a higher rate.[1] Moreover, these materials can cover almost arbitrarily curved surfaces and movable parts.[2] Flexible dielectrics are being used extensively in electronic control systems, on board computers, consumer electronics, heart pacemakers, and as dielectric waveguides.[3,4] Considerable efforts have been devoted to the design and characterization of dielectric wave guides for microwave frequencies.[5] Rectangular wave guides made from dielectric materials have proven to be a very capable alternative to conventional metal waveguides and quasi optical waveguide assemblies because of their low attenuation, bending flexibility and rather low cost of manufacture. The demand for flexible, low attenuation waveguides at sub-millimetre wave frequencies is on the increase.[6] The requirements for a material to be used as a flexible dielectric waveguide are mechanical flexibility, high relative permittivity, low dielectric loss, low coefficient of thermal expansion (CTE) etc. It is very difficult to identify a single material which possesses these properties simultaneously. There are a number of ceramic materials with high relative permittivity and low dielectric loss. However, processibility of the ceramics is poor due to their brittle nature. There are several low loss polymers with good mechanical flexibility but they have low relative permittivity and high CTE. Therefore, the application of a flexible polymer alone or a ceramic alone is limited.[7] By integrating the flexibility and low processing temperature of a polymer with high relative permittivity and low loss of ceramics, a composite may be formed, which can deliver improved performances.[8]

Several authors have reported results on the preparation and properties of elastomer–ceramic composites and polymer–ceramic composites.[9–12] Recently Thomas et al. reported the microwave dielectric properties of butyl rubber–strontium titanate composite. This composite showed a relative permittivity (ε_r) of 13.2 and a dielectric loss (tan δ) of 2.8×10^{-3} at 5 GHz for a volume fraction 0.42 of the ceramic.[13] Ward et al. reported the effect of stress–strain cycles on the dielectric properties of butyl rubber vulcanizates filled with silica using dielectric spectroscopy. The dielectric properties were not found to change after storage at room temperature even for a year.[14]

Correspondence to: M. T. Sebastian (mailadils@yahoo.com).

Contract grant sponsor: Department of Science and Technology.

TABLE I
Formulations of the Composites Used

Ingredients in phr[a]	BS-0	BS-1	BS-2	BS-3	BS-4	BS-5
Butyl rubber	100	100	100	100	100	100
Stearic acid	3	3	3	3	3	3
Zinc oxide	5	5	5	5	5	5
Tetramethylthiuram disulfide (TMTD)	1	1	1	1	1	1
Sulfur	0.5	0.5	0.5	0.5	0.5	0.5
$Sr_2Ce_2Ti_5O_{15}$ (SCT)[b]	0 (0)	50 (0.09)	100 (0.16)	200 (0.27)	300 (0.36)	400 (0.43)

[a] Parts per hundred parts of rubber.
[b] The corresponding SCT volume fraction is given in parenthesis.

Even though studies have been reported on ceramic filled rubber composites, only a few reports are available in literature which explores the potential of rubber composites for flexible wave guide applications.[7,13] Among various elastomer materials, butyl rubber has excellent dielectric properties, such as low relative permittivity ($\varepsilon_r \approx 2.4$) and low dielectric loss (tan $\delta \approx 10^{-3}$), mechanical flexibility, good weathering resistance, biocompatibility etc.[9] Recently $Sr_{2+n}Ce_2Ti_{5+n}O_{15+3n}$ (n = 0–10) based ceramics and their composites has been studied extensively due to their high relative permittivity and relatively low dielectric loss.[15–19] $Sr_2Ce_2Ti_5O_{15}$ (SCT) ceramic has a high relative permittivity of 112, low loss of 10^{-4} at 7 GHz and a low CTE of 1.7 ppm $^{\circ}C^{-1}$.[15,16] The high permittivity of the SCT ceramics limits the amount of the filler to achieve maximum ε_r for the flexible composites. The synthesis, dielectric and thermal properties of butyl rubber–$Sr_2Ce_2Ti_5O_{15}$ (BS) composites are reported in the present article.

EXPERIMENTAL

$Sr_2Ce_2Ti_5O_{15}$ ceramic powder was prepared following the conventional solid state ceramic route. Stoichiometric quantities of $SrCO_3$ and TiO_2 (99.9 + %, Sigma-Aldrich) and CeO_2 (99.99%, Indian Rare Earths) were ball milled for 24 h in distilled water using Yttria-stabilized Zirconia balls in a plastic container. The slurry was dried and calcined at 1100°C for 4 h. The calcined powder was ground well and sintered at 1300°C for 4 h. The powder was then sieved through a 25-μm sieve. Butyl rubber–$Sr_2Ce_2Ti_5O_{15}$ (BS) composites were prepared by sigma mixing. The compositions for BS-0, BS-1, BS-2, BS-3, BS-4, and BS-5 are given in Table I.[20] In rubber based compounds the accepted practice is to use parts per hundred parts of rubber (phr) to quantify the ingredients used for vulcanization. However, in the theoretical modeling of properties of the composites and other calculations it is convenient to specify the filler content in volume fraction. Therefore the volume fractions of the SCT filler are also given in Table I. The mixing was done in a kneading machine. Kneading machine is a variable speed mixer having two counter rotating sigma blades with a gear ratio 1:2. The uniform mixtures so obtained were then hot pressed at 200°C for 90 min under a pressure of 2 MPa.

The phase purity of the ceramic powder was analyzed by recording the X-ray powder diffraction pattern with Cu Kα radiation (Philips X'Pert PRO MPD X-ray diffractometer). Glass transition temperatures (T_g) of the composites were measured with a differential scanning calorimeter (Metler Toledo Model, DSC 822[e]) keeping a heating rate of 10°C min^{-1}. Tensile tests on the BS composites were conducted using dumb-bell shaped samples of width ≈ 4 mm and thickness in the range 1.5–2 mm. The measurements were carried out in a Universal Testing Machine (Hounsfield Model, H5K-S UTM) with a rate of grip separation of 500 mm min^{-1}. The microstructures of the composites were examined using a Scanning Electron Microscope (SEM) (Jeol Model, JSM 5600LV). The dielectric properties at 1 MHz were measured following the parallel plate capacitor method using a LCR meter (Hioki Model, 3532-50). Dielectric sheets of dimensions 30 mm × 30 mm and thickness of about 1.8 mm were used for the microwave measurements. The microwave dielectric properties were measured using a split post dielectric resonator (SPDR) with the help of a vector network analyzer (Agilent Model, 8753ET). The SPDR operating at 5.155 GHz requires the above mentioned dimensions for accurate measurement.[21] An improved photopyroelectric (PPE) technique[22–24] was used to determine the thermal conductivity of the BS composites. A 70 mW He-Cd laser with a wavelength of 442 nm, intensity modulated by a mechanical chopper (SRS Model, SR540), was used as the optical heating source. A PVDF film with a thickness of 28 μm with Ni-Cr coating on both sides was used as the pyroelectric detector. The output signal was measured with a lock-in amplifier (SRS Model, SR 830). The modulation frequency was kept above 60 Hz to ensure that the detector, sample, and the backing medium were all thermally thick during the

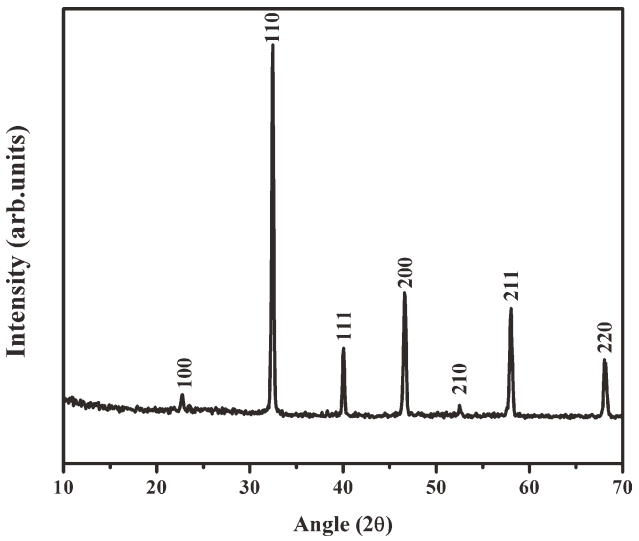

Figure 1 X-ray diffraction pattern of SCT.

measurements. In the experiment we measured the variations of the pyroelectric signal amplitude and phase with modulation frequency. The thermal diffusivity and thermal effusivity of the samples were then derived from these. From the values of thermal diffusivity and thermal effusivity, the thermal conductivity and specific heat capacity of the samples were calculated. The linear coefficient of thermal expansion of each composite was measured using a dilatometer (Netzsch Model, DIL 402 PC). The moisture absorption characteristics of the composites were measured by following the ASTM D 570-98 procedure.[25] The samples with dimensions 50 mm × 50 mm × 2 mm were weighed accurately and immersed in distilled water for 24 h. The samples were then taken out and again weighed after removing the excess water from the surface. The volume % of water absorption was then calculated using the relation,

$$\text{Volume \% water absorption} = \frac{(W_f - W_i)/\rho_w}{(W_f - W_i)/\rho_w + W_i/\rho_c} \times 100 \quad (1)$$

where w_i and w_f are the initial and final weights of the sample and ρ_w and ρ_c are the densities of distilled water and sample, respectively.

RESULTS AND DISCUSSION

Figure 1 shows the powder XRD pattern of pure $Sr_2Ce_2Ti_5O_{15}$ (SCT) sintered at 1300°C for 4 h. All the peaks are indexed based on previous reports.[15,16] The formation of phase pure SCT is obvious from Figure 1.

Figure 2 shows the DSC thermogram of BS composites. Differential scanning calorimetry technique

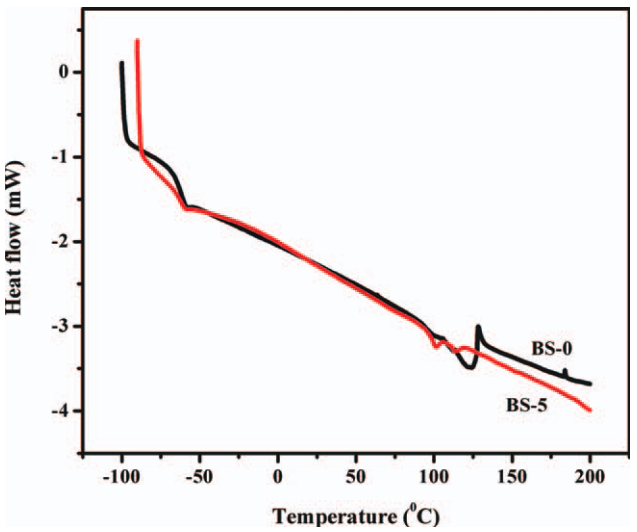

Figure 2 DSC thermogram of BS composites. [Color figure can be viewed in the online issue, which is available at wileyonlinelibrary.com.]

has been used for the determination of glass transition temperature of polymers. The unloaded rubber shows an endothermic peak at −63°C corresponding to its glass transition temperature. The composite with maximum filler loading with volume fraction (v_f) 0.43 also shows a peak at the same temperature indicating that there is no significant change in glass transition temperature even after maximum filler loading in these samples.

Figure 3 shows the stress- strain curves of BS composites. The samples do not break even up to an elongation of 1000%. It has been reported that the stress–strain curves for particle filled rubber systems are affected by the crosslink density of the rubber matrix, the size of agglomerates and rubber–filler

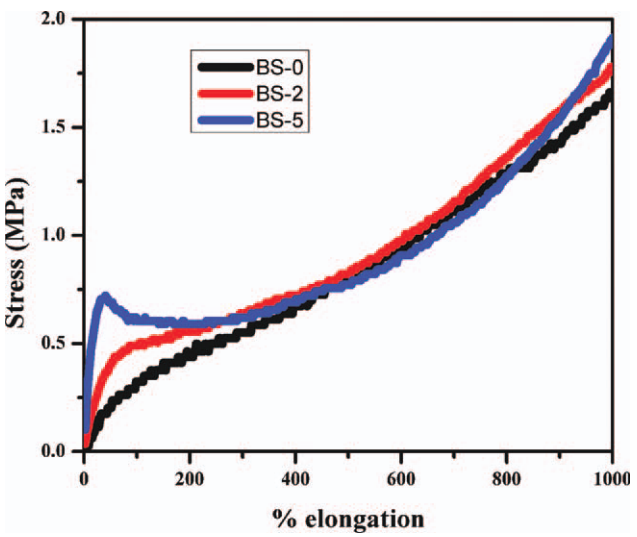

Figure 3 Stress strain curves of BS composites. [Color figure can be viewed in the online issue, which is available at wileyonlinelibrary.com.]

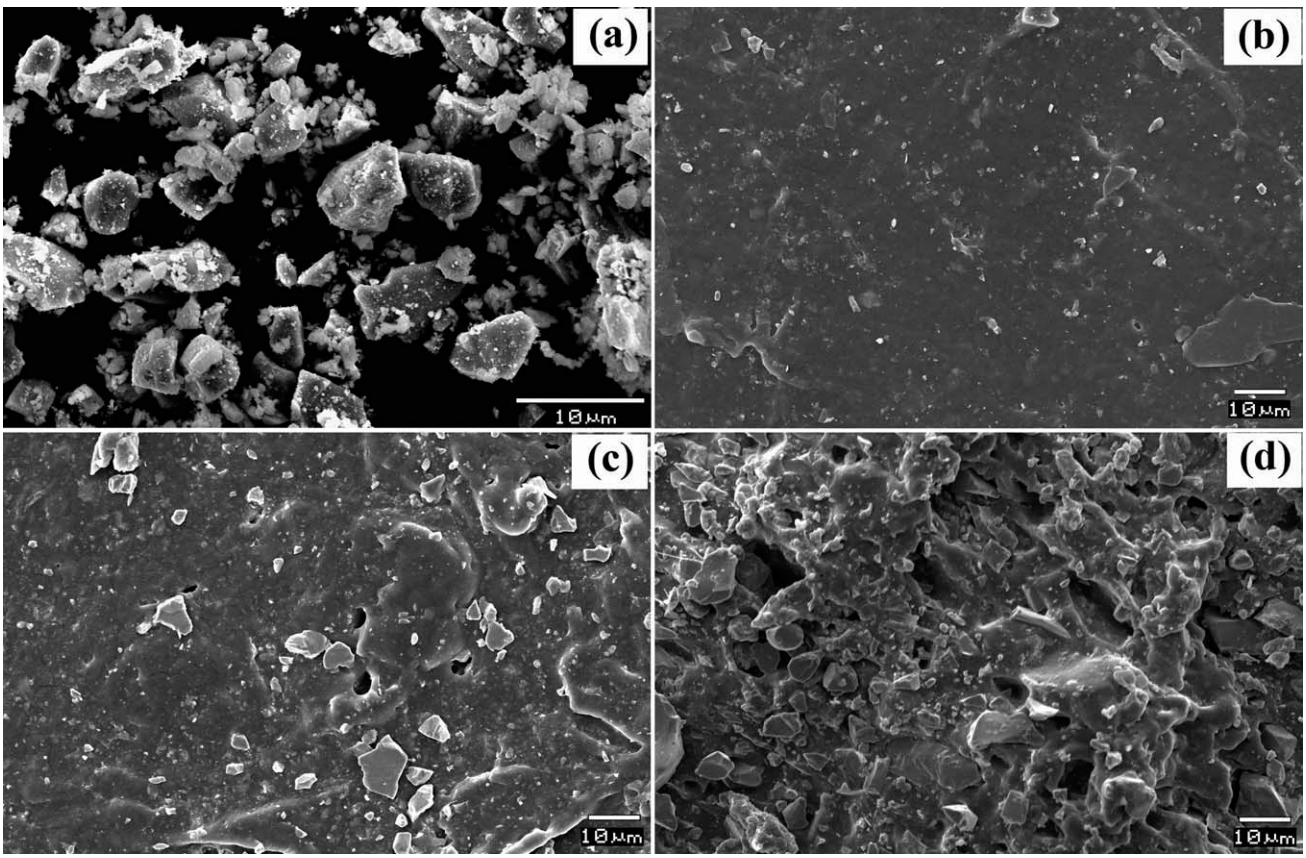

Figure 4 SEM of (a) SCT, (b) BS-1, (c) BS-5, and (d) fractured BS-5.

interactions.[26,27] It is clear from Figure 3 that the stress required for elongation increases with filler loading. This indicates that stiffness of the composites increases with filler contents. However, the composites are flexible enough and remain unbroken up to a strain of 1000%.

Figure 4(a) shows the SEM image of the pure SCT powder. The particles are irregularly shaped with size less than about 10 μm. The surface morphology of BS-1 and BS-5 composites are depicted in Figure 4(b) and (c), respectively. It can be seen that for low filler loading, the ceramic particles are uniformly distributed in the rubber matrix. As the filler content increases particle agglomeration occurs and porosity arises, which can be seen in Figure 4(c). Figure 4(d) shows SEM image of the fractured surface of the BS-5 composite. It is clear from the Figure 4(d) that there is good adhesion between the filler and the matrix.

Figure 5 shows the variation of relative permittivity of BS composites with filler loading at 1 MHz and 5 GHz. The value of ε_r increases with filler loading because ε_r of the filler is relatively high (112 at 7 GHz). At 1 MHz, the relative permittivity increases from 2.4 to 8.8, and at 5 GHz it increases from 2.4 to 11.9. The relative permittivity of the composites is also affected by a number of factors such as the porosity, size and shape of the filler particles, interface between the components and the effective dipole moment of the composites.[28] At lower volume fractions, since the high permittivity ceramic is a minor dispersed phase, the major contribution to the dielectric response comes from the continuous rubber matrix. As the filler loading increases the

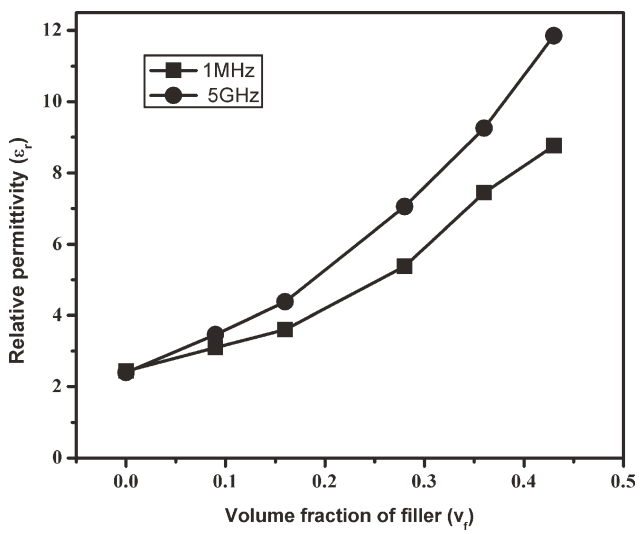

Figure 5 Variation of relative permittivity with filler loading.

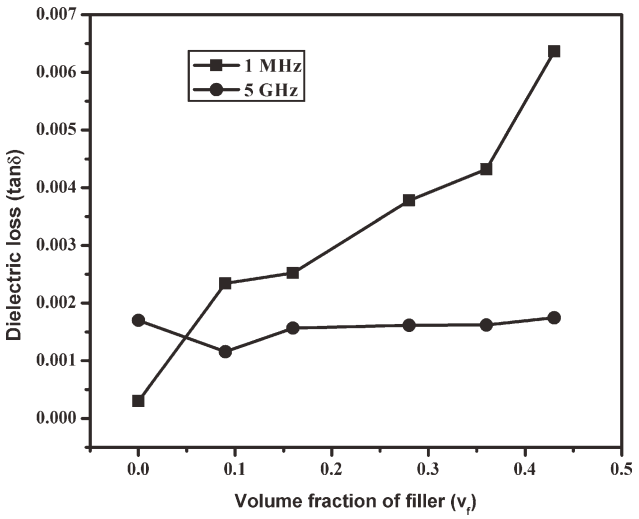

Figure 6 Variation of dielectric loss with ceramic content.

ceramic particles form continuous networks and the dipole–dipole interaction increases. Consequently there will be a rise in relative permittivity of the composite.[29]

Figure 6 shows the variation of the dielectric loss of BS composites with the filler volume fraction at 1 MHz and 5 GHz. As volume fraction of SCT increases, tan δ increases from 3×10^{-4} to 6.4×10^{-3} at 1 MHz, and from 1.7×10^{-3} to 1.8×10^{-3} at 5 GHz, respectively. The loss factor increases at both the frequencies, although the variation is marginal at 5 GHz. The dielectric loss of a composite is affected by extrinsic factors such as porosity, microstructure, moisture content, and interface between the polymer and the filler. A dense composite with low moisture content is needed for obtaining a low loss composite. With increase in filler volume fractions the space charge getting accumulated in the interfacial area increases, leading to an increase in dielectric loss. However, this interfacial effect is effective only at low frequencies.[30] Hence the increase in tan δ with filler volume fraction is more significant at 1 MHz than at microwave ranges.

The temperature dependence of ε_r at 1 MHz is depicted in Figure 7. For most of the practical applications, the relative permittivity of the materials should be stable within the operational temperature range of the electronic devices. The relative permittivity of the composites with lower filler loading is almost constant throughout the measured temperature range. As the filler loading increases there is a decrease in relative permittivity with temperature. This may be due to the incipient ferroelectric nature of SCT. Incipient ferroelectrics are characterized by increasing permittivity on cooling due to the softening of the lowest frequency polar optical phonon.[17] Recently Subodh et al. have reported a similar behavior in polyethylene–$Sr_9Ce_2Ti_{12}O_{36}$ composites.[18]

To understand the physical mechanisms controlling the relative permittivity of a heterogeneous system, the experimental values of ε_r were compared with values predicted using different theoretical models. Figure 8 displays a comparison of the experimental relative permittivity of BS composites at 5 GHz with that obtained using Maxwell–Garnet equation, Lichtnecker equation, Jayasundere–Smith equation and the Effective medium theory (EMT), which are all reproduced below.[8]

$$\frac{\varepsilon_{\text{eff}} - \varepsilon_m}{\varepsilon_{\text{eff}} + 2\varepsilon_m} = v_f \frac{\varepsilon_f - \varepsilon_m}{\varepsilon_f + 2\varepsilon_m} \quad \text{(Maxwell-Garnet Equation)} \tag{2}$$

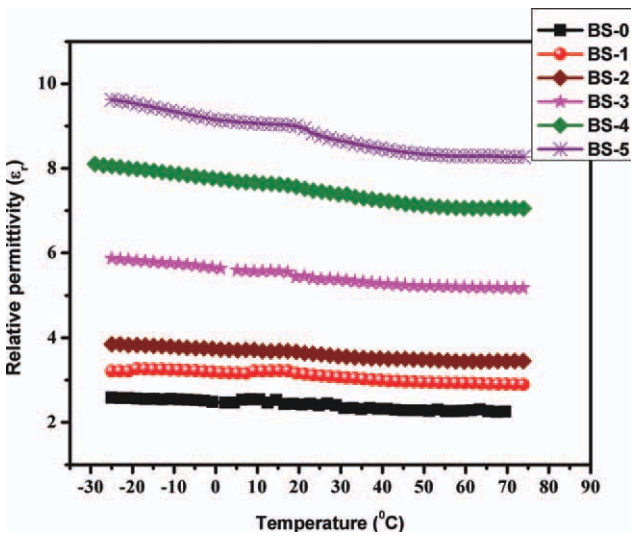

Figure 7 Temperature dependence of relative permittivity. [Color figure can be viewed in the online issue, which is available at wileyonlinelibrary.com.]

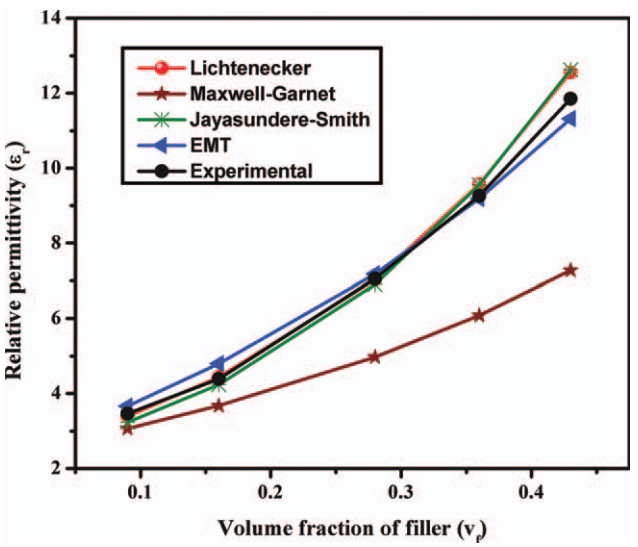

Figure 8 Comparison of experimental and theoretical ε_r. [Color figure can be viewed in the online issue, which is available at wileyonlinelibrary.com.]

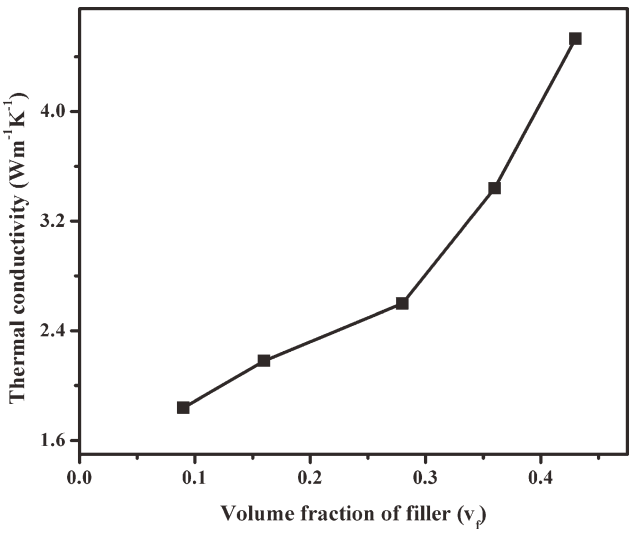

Figure 9 Thermal conductivity variation with ceramic content.

$$\ln \varepsilon_{\text{eff}} = (1 - v_f) \ln \varepsilon_m + v_f \ln \varepsilon_f$$

(Lichtennecker Equation) (3)

$$\varepsilon_{\text{eff}} = \frac{\varepsilon_m(1 - v_f) + \varepsilon_f v_f \left[\frac{3\varepsilon_m}{\varepsilon_f + 2\varepsilon_m}\right]\left[1 + \frac{3v_f(\varepsilon_f - \varepsilon_m)}{(\varepsilon_f + 2\varepsilon_m)}\right]}{(1 - v_f) + v_f \left[\frac{3\varepsilon_m}{\varepsilon_f + 2\varepsilon_m}\right]\left[1 + \frac{3v_f(\varepsilon_f - \varepsilon_m)}{(\varepsilon_f + 2\varepsilon_m)}\right]}$$

(Jayasundere-Smith Equation) (4)

$$\varepsilon_{\text{eff}} = \varepsilon_m \left[1 + \frac{v_f(\varepsilon_f - \varepsilon_m)}{\varepsilon_m + n(1 - v_f)(\varepsilon_f - \varepsilon_m)}\right]$$

(Effective Medium Thoery) (5)

where ε_{eff}, ε_f, and ε_m are the relative permittivity of the composite, filler and matrix, respectively. (v_f) is the volume fraction of the filler and n is a shape factor. It is clear from Figure 8 that the values of ε_r obtained using Maxwell–Garnet formula shows considerable deviation from the experimental values. This relation is suitable for very low volume fraction of ceramic particles. For higher particle loading, there is reduction in depolarization of fillers and increase in relative permittivity, which are not accounted for in this formula.[31] The most widely used relation for the prediction of ε_r is Lichtenecker's logarithmic law of mixing. It considers the composite system as randomly oriented spheroids that are uniformly distributed in a continuous matrix. In the present study, this equation fits well with experimental values except at higher filler loadings. This may be due to the agglomeration of ceramic particles at higher filler loading.[32] It is obvious from Figure 8 that Jayasundere–Smith equation is also suitable for the prediction of ε_r. This equation is a modification of well-known Kerner equation by including the interactions.[33] This equation considers composite as a bi-phase system of dielectric spheres (ε_f) dispersed in a continuous medium (ε_m) and is valid only when $\varepsilon_f > \varepsilon_m$. Even though most of the above mentioned equations fit with experimental values of ε_r, a good matching is obtained with the Effective Medium Theory (EMT) developed by Rao et al.[34] This model considers a shape factor n. The shape factor n used for SCT ceramic is 0.165. This is in agreement with an earlier report.[32] In EMT model composites are treated as an effective medium whose relative permittivity is obtained by averaging over the relative permittivity of the constituents. The basic concept of EMT model is that when a random unit cell (RUC) is embedded in an effective medium it cannot be detected in the electromagnetic experiment. A random unit cell is defined as a core of ceramic surrounded by a concentric shell of the polymer.

Heat dissipation is a major problem in microelectronic devices and circuits. To overcome this problem, substrates with high thermal conductivity are to be used. Heat conduction in solids is by the transport of heat energy carried by lattice vibrations or phonons. The very low thermal conductivity of polymers is due to the scattering of phonons by the complex chain network and the lack of crystallinity of the polymer.[35] Ceramic fillers seem to improve the thermal conductivity of polymer chains as they act as conducting channels with lower thermal resistance than the matrix. Figure 9 shows the variation of thermal conductivity of BS composites with filler loading. As the filler content increases, thermal conductivity of the composite also increases, and reaches a value 4.5 Wm^{-1} K^{-1} for maximum filler content with volume fraction 0.43. At still higher filler loadings, thermally conductive networks were

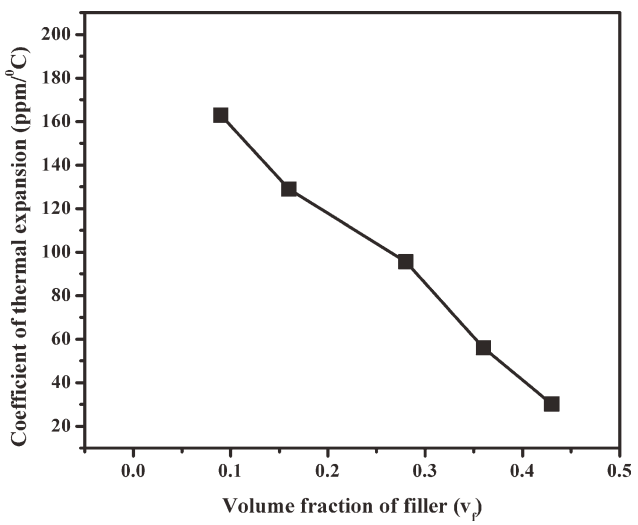

Figure 10 Variation of CTE of the composites with SCT content.

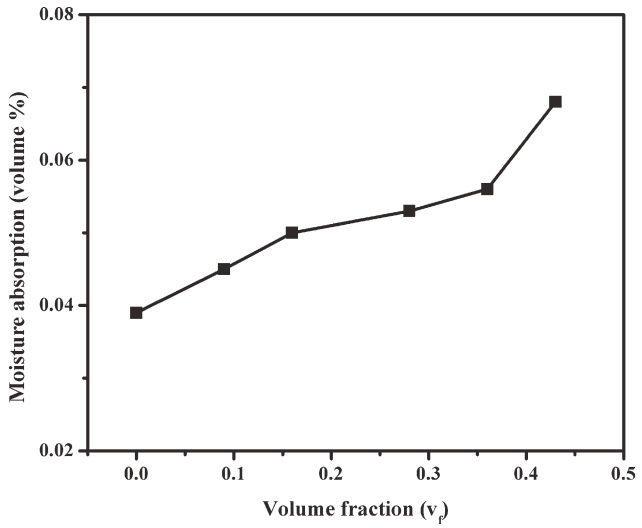

Figure 11 Variation of moisture absorption with ceramic loading.

formed throughout the system and this leads to the rise in thermal conductivity of the composites.

Figure 10 shows the variation of coefficient of thermal expansion (CTE) of BS composites with filler loading. The large value of CTE of polymers is caused by the low energy barrier for the chain conformation to be changed and this high CTE precludes polymers from practical applications.[36] It is clear from Figure 10 that the CTE of pure butyl rubber (191 ppm $^{\circ}C^{-1}$)[13] is very much reduced by the addition of ceramic filler (SCT) which is having a very low CTE of 1.7 ppm $^{\circ}C^{-1}$. The increase in filler volume fraction results in decreased free volume of polymer and hence reduced room for polymer expansion.[37] The CTE of the BS-5 composite with volume fraction 0.43 of filler is 30.2 ppm $^{\circ}C^{-1}$.

Moisture absorption is a major concern in polymer–ceramic composites when it comes to practical applications. The water content deleteriously influences the dielectric properties of composites.[38] Figure 11 shows the moisture absorption of the composites with ceramic loading. Moisture penetration into composites takes place mainly through diffusion along the matrix–filler interface and through the pores. As the ceramic loading increases, the moisture content also increases. This may be due to increased porosity at higher filler loading as evident from the SEM images (Fig. 4). One of the reasons for the rise in relative permittivity and dielectric loss (Figs. 5 and 6) with filler loading may be the presence of moisture.

CONCLUSION

Mechanically flexible butyl rubber–strontium cerium titanate (BS) composites were prepared. The dielectric properties of the composites were investigated at 1 MHz and 5 GHz. The relative permittivity and dielectric loss for the BS-5 were measured to be 11.8 and 1.8×10^{-3}, respectively at 5 GHz. The thermal properties such as CTE and thermal conductivity of the BS composites were found to improve by the addition of SCT content. The CTE of the composites got reduced to 30.2 ppm $^{\circ}C^{-1}$ and thermal conductivity increased to 4.5 Wm^{-1} K^{-1} for volume fraction 0.43 of SCT content. The measured properties indicate that the BS composite is suitable for application as flexible substrates as well as wave guides at microwave frequencies.

The authors are thankful to Dr. U. Shyamaprasad and Mr. P. Guruswamy for recording XRD pattern, Dr. P. Prabhakar Rao and Mr. M. R. Chandran for SEM, and Mr. Brahmakumar for tensile measurements.

References

1. Nathan, A.; Chalamala, B. R. Proc IEEE 2005, 93, 1235.
2. Siegel, A. C.; Phillips, S. T.; Dickey, M. D.; Lu, N.; Suo, Z.; Whitesides, G. M. Adv Funct Mater 2010, 20, 28.
3. Friend, R. H.; Gymer, R.; Holmes, A. B.; Burroughes, J. H.; Marks, R. N.; Taliani, C.; Bradley, D. D. C.; Santos, D. A. D.; Brédas, J. L.; Lögdlund, M.; Salaneck, W. R. Nature 1999, 397, 121.
4. Lappas, A.; Zorko, A.; Wortham, E.; Das, R. N.; Giannelis, E. P.; Cevc, P.; Arcon, D. Chem Mater 2005, 17, 1199.
5. Obrzut, J.; Goldsmith, P. F. IEEE Trans Microwave Theory Tech 1990, 38, 324.
6. Hofmann, A.; Horster, E.; Weinzierl, J.; Schmidt, L. P.; Brand, H. 33rd Eur Microwave Conf 2003, 955.
7. Xiang, F.; Wang, H.; Yao, X. J Eur Ceram Soc 2007, 27, 3093.
8. Sebastian, M. T.; Jantunen, H. Int J Appl Ceram Technol 2010, 7, 415.
9. Hakim, I. K.; Bishai, A. M.; Saad, A. L. J Appl Polym Sci 1988, 35, 1123.
10. Koulouridis, S.; Kiziltas, G.; Zhou, Y.; Hansford, D. J.; Volakis, J. L. IEEE Trans Microwave Theory Tech 2006, 54, 4202.
11. Sumesh, G.; Sebastian, M. T. J Appl Polym Sci 2009, 114, 1682.
12. Yang, R.; Wong, C. P. J Appl Polym Sci 2004, 92, 2228.
13. Thomas, D.; Janardhanan, C.; Sebastian, M. T. Int J Appl Ceram Technol 2010. DOI:10.1111/j.1744-7402.2010.02584.x.
14. Ward, A. A.; Stoll, B.; Soden, W. V.; Herminghaus, S.; Bishai, A. M.; Hanna, F. F. J Macromol Sci Part B Phys B 2003, 42, 1265.
15. Subodh, G.; Sebastian, M. T. Mater Sci Eng B 2007, 136, 50.
16. Subodh, G.; James, J.; Sebastian, M. T.; Paniago, R. M.; Dias, A.; Moreira, R. L. Chem Mater 2007, 19, 4077.
17. Kamba, S.; Savinov, M.; Laufek, F.; Tkac, O.; Kadlec, C.; Veljko, S.; John, E. J.; Subodh, G.; Sebastian, M. T.; Klementova, M.; Bovtun, V.; Pokorny, J.; Goian, V.; Petzelt, J. Chem Mater 2009, 21, 811.
18. Subodh, G.; Deepu, V.; Mohanan, P.; Sebastian, M. T. Appl Phys Lett 2009, 95, 062903–1.
19. Subodh, G.; Deepu, V.; Mohanan, P.; Sebastian, M. T. J Phys D Appl Phys 2009, 42, 225501.
20. Barron, H. Modern Synthetic Rubbers; Chapman & Hall: London, 1949.
21. Sebastian, M. T. Dielectric Materials for Wireless Communications, 1st ed.; Elsevier: Oxford, UK, 2008.
22. Menon, C. P.; Philip, J. Meas Sci Technol 2000, 11, 1744.
23. Marinelli, M.; Murtas, F.; Mecozzi, M. G.; Martellucci, S. Appl Phys A Mater Sci Process 1990, 51, 387.
24. Sebastian, M. T.; Menon, C. P.; Philip, J.; Schwartz, R. W. J Appl Phys 2003, 94, 3206.

25. Anjana, P. S.; Deepu, V.; Uma, S.; Mohanan, P.; Philip, J.; Sebastian, M. T. J Polym Sci Polym Phys 2010, 48, 998.
26. Yatsuyanagi, F.; Suzuki, N.; Ito, M.; Kaidou, H. Polym J 2002, 34, 332.
27. Suzuki, N.; Yatsuyanagi, F.; Ito, M.; Kaidou, H. J Appl Polym Sci 2002, 86, 1622.
28. Chen, Y. C.; Lin, H. C.; Lee, Y. D. J Polym Res 2003, 10, 247.
29. Kuo, D. H.; Chang, C. C.; Su, T. Y.; Wang, W. K.; Lin, B. Y. Mater Chem Phys 2004, 85, 201.
30. Smaoui, H.; Mir, L. E. L.; Guermazi, H.; Agnel, S.; Toureille, A. J Alloys Comp 2009, 477, 316.
31. Rajesh, S.; Murali, K. P.; Rajani, K. V.; Ratheesh, R. Int J Appl Ceram Technol 2009, 26, 553.
32. Subodh, G.; Pavithran, C.; Mohanan, P.; Sebastian, M. T. J Eur Ceram Soc 2007, 27, 3039.
33. Poon, Y. M.; Shin, F. G. J Mater Sci 2004, 39, 1277.
34. Rao, Y.; Qu, J.; Marinis, T.; Wong, C. P. IEEE Trans Compon Packag Technol 2000, 23, 680.
35. Zhou, W.; Qi, S.; Tu, C.; Zhao, H. J Appl Polym Sci 2007, 104, 2478.
36. Rao, Y. Q.; Blanton, T. N. Macromolecules 2008, 41, 935.
37. Goyal, R. K.; Tiwari, A. N.; Mulik, U. P.; Negi, Y. S. Compos Sci Technol 2007, 67, 1802.
38. Tsenoglou, C. J.; Pavlidou, S.; Papaspyrides, C. D. Compos Sci Technol 2006, 66, 2855.